NJC

PAPER

View Article Online
View Journal | View Issue

Check for updates

Cite this: *New J. Chem.*, 2017, **41**, 13576

# Noncovalently bound complexes of polar molecules: dipole-inside-of-dipole *vs.* dipole–dipole systems†

S. Kerr and F. Y. Naumkin *

Received 27th July 2017,
Accepted 28th September 2017

DOI: 10.1039/c7nj02753b

rsc.li/njc

A series of molecular complexes including the uncommon M-mol-X species with one molecule (fluorocarbon) trapped between fragment counter-ions of the other (alkali halide MX), are compared to the usual mol-MX conformers with molecules attached to one another. The systems are characterized in terms of structures and stabilities, charge distributions and dipole moments, IR intensity spectra and electron attachment. Significant variations in the relative stabilities of the conformers are found between the systems with trapped-molecule isomers of different polarity as well as between neutral systems and their anions. In particular, it is shown that the M-mol-X conformers can be degenerate or perhaps even more stable relative to the mol-MX ones, as well as that the higher-energy isomer of the molecule can form a more stable complex. The electron-attachment is predicted to favour production of such uncommon species experimentally *via* making them very close in energy to the usual complexes and lowering the relevant energy barriers. The systems are highly polar and their IR intensity spectra are demonstrated not only to sensitively indicate the complex formation, but also to distinguish the specific conformers. The predicted features are hoped to aid experimental detection of novel species.

## Introduction

Polyatomic molecules have multiple stable isomers with different properties depending on their structures. Higher-energy isomers can have interesting properties, so it is important to explore their variety in order not to overlook attractive alternatives in favour of stability alone. Indeed, the ground isomer is just one such, with a rich multitude of others on top. In particular, polarity is one such property of interest, determining, *e.g.*, the intensity of the interactions with light and facilitating relevant applications, including solar cells, lasers, and in optoelectronics.[1,2] Other uses are based on the stronger interactions between polar molecules, assisting, for instance, efficient complexation, self-assembly and reactivity.

A good example involving the aspects mentioned above is the recently synthesized molecule of all-*cis* (1,2,3,4,5,6-fluorinated) cyclic $C_6H_6F_6$, with only hydrogen on one face of the carbon ring and only fluorine on the other.[3] It has a record-level (for covalently bonded molecules) dipole moment of about 6 D, while being a high-energy isomer. This does confirm that an interest in a molecule because of its anticipated unique properties can cause attention and stimulate efforts, leading to the development of an experimental procedure for producing it – regardless of its higher energy relative to other isomers.

The high polarity leads to considerable stabilities of the molecule's complexes with ions,[4–6] in particular studied experimentally for $Na^+$ and $Cl^-$,[4] and with other polar molecules such as alkali halides.[5] As an ultimate case, the systems of stretched ionic (*e.g.* alkali-halide) diatoms with the molecule inserted between the counter-ions show significant stabilities (up to about 1 eV) relative to the separated components, as well as very large dipole moments (up to about 20 D).[5,6] One consequence of the latter is very high IR intensities at specific wavelengths corresponding to the axial vibrations in the system – mainly of the molecule in the electric field of the framing counter-ions.[6]

Similar features have been predicted for analogous systems of nonpolar hydrocarbons such as cyclic $C_6H_{12}$ trapped between the counter-ions,[6,7] even though less stable to dissociation (in fact, metastable, *i.e.* higher in energy than the separate components and stabilized by an energy barrier). Other similar systems include counterparts with smaller cyclic molecules such as all-*cis* $C_3H_3F_3$ and $C_4H_4F_4$[8] in addition to their non-fluorinated parents, $C_3H_6$ and $C_4H_8$,[9,10] all-fluorinated ethane[11] as well as benzene and its derivatives (see ref. 12 and 13, recent reviews[14,15] and references therein). The above nonpolar molecules, however, are characterized by the rather low energy barriers stabilizing the corresponding metastable systems relative to dissociation, while the polar species are more stable due to the strong ion–dipole interactions.

---

*Faculty of Science UOIT Oshawa, ON, L1H 7K4 Canada.*
*E-mail: Fedor.Naumkin@uoit.ca*

† Electronic supplementary information (ESI) available. See DOI: 10.1039/c7nj02753b

It is thus of interest to expand the family of such systems and to identify the most stable ones. In particular, the feasibility of experimentally producing all-*cis* $C_4H_4F_4$ is supported by the success in making the larger $C_6H_6F_6$ counterpart as well as tetrafluorinated all-*cis* cyclic $C_5H_6F_4$ and $C_6H_8F_4$.[16–18] The earlier work investigated a series of M–$C_4H_4F_4$–X systems (M = Li to K, X = F to Br) and predicted them to be stable to dissociation into MX + $C_4H_4F_4$ by up to 0.4 eV.[8] Previously, the analogous M–$C_6H_6F_6$–X (MX = LiF to KBr, CsCl, CsI) and M–$C_4H_8$–X (M = Li, Cs; X = Cl, I) systems were found to be most stable for MX = CsI,[5,6,10] apparently due to the largest diatom being least perturbed by insertion of the molecule. In addition, the M–$C_4H_8$–X stabilities to dissociation into molecular components increased upon electron attachment.[10] Therefore the present work focusses on CsI in combination with a few isomers of $C_4H_4F_4$ (including the higher-energy all-*cis* one) of different polarity, for both neutral complexes and their anions.

## Theoretical methods and tools

In accord with the noncovalent character of the interactions governing the system, *ab initio* calculations have been performed at the MP2 level of theory with the extensive aug-cc-pVTZ basis sets for light atoms (H, C, F), and the Stuttgart's relativistic effective core potentials and associated basis sets for Cs and I.[19] All these are implemented in the NWChem suit of programs[20] employed in this work.

The accuracy of calculations with this setup has been verified *via* comparison of predicted and experimental parameters such as ionization energy and electron affinity for atoms, equilibrium internuclear distances, dissociation energies and dipole moments for constituent diatoms. In particular, IE(Cs) = 3.75 eV and EA(I) = 3.14 eV are close to the experimental 3.89 and 3.06 eV, respectively, and the deviations are sufficiently small for the diatoms as well (Table 1).

Full geometry optimizations have been followed by vibrational frequency analyses to differentiate the true energy minima and transition states, and to re-optimize the latter using the corresponding eigenvectors. Atomic charges have been determined using the natural bonding orbital approach.[23] The IR intensities have been calculated by means of NWChem as well.

## Results and discussion

### Structures and stabilities

Table 1 Equilibrium parameters[a] of ion-pair diatoms

| MX | $D_e$/eV | $R_e$/Å | $\mu_e$/D |
|---|---|---|---|
| CsI | 3.59 (3.51 ± 0.02) | 3.38 (3.32) | 12.3 (11.7) |
| CsF | 5.55 (5.38 ± 0.08) | 2.38 (2.35) | 8.17 (7.88) |
| HI | 3.41 (3.09) | 1.59 (1.61) | 0.42 (0.45) |

[a] Bracketed values are experimental data.[21,22]

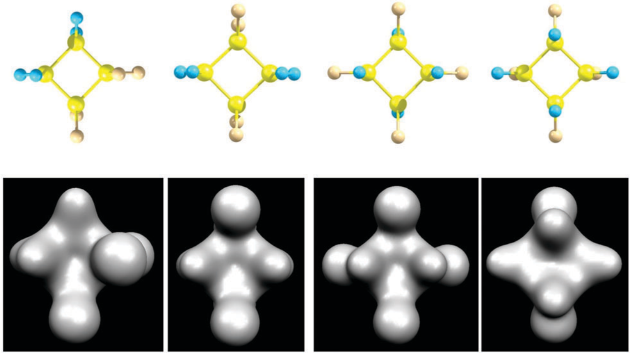

Fig. 1 Optimized geometries of the 11′22′-, 11′33′- (*cross*), 12′34′- and 1234- (all-*cis*) isomers of $C_4H_4F_4$, and their electron densities (cutoff of 0.05 a.u.).

Shown in Fig. 1 are four isomers of $C_4H_4F_4$, different in the positions of the substituting F atoms and selected in terms of relative stability as discussed in the following. The 11′22′- and 11′33′-isomers are lowest in energy and commercially available, while the 12′34′- and 1234-isomers are higher-energy ones while symmetric and could thus favour the formation of the insertion complexes. However, it is found that the 11′22′- and 12′34′-isomers do not form insertion complexes with CsI, and the framing Cs and I slide around the molecule and recombine into a diatom attached by polarization. The former case can be readily understood in terms of the asymmetry of the electron density in 11′22′-$C_4H_4F_4$, which is larger on the fluorine side and lower on the hydrogen side (Fig. 1), thus producing a destabilizing gradient of electrostatic interactions. For this reason, other asymmetric isomers are not considered here. The other isomer is more symmetric, but its charge distribution may still destabilize the framing ion-pair, allowing its shift as a whole (keeping the Cs–I distance to avoid an increase of energy) from the axial positions sideways (vertically or horizontally in the picture). Then $Cs^+$ would move towards one of the (partly anionic) F's and $I^-$ towards the corresponding (partly cationic) H on the opposite face of the carbon ring, thus lowering the energy. Still another symmetric $C_4H_4F_4$ with the 1′23′4 substitution scheme is unstable and relaxes to the 12′34′ isomer.

On the other hand, each of the 11′33′- and 1234-isomers of $C_4H_4F_4$ does get trapped between Cs and I in an aligned geometry (Fig. 2 and 3), with Cs on the F side and I on the H side, with near-equal Cs–F and H–I distances, especially for the latter case (Table 2). In particular, if Cs and I are added on the opposite sides, the 11′33′-$C_4H_4F_4$ molecule inverts, recovering the previous arrangement. In the following, only the systems with the 11′33′- (hereafter *cross*) and 1234-(all-*cis*) isomers of $C_4H_4F_4$ are considered.

In particular for the former case, while the electron densities facing each of the Cs and I are similar to those for 11′22′-$C_4H_4F_4$ (but not staggered), the charge distribution in the *cross*-$C_4H_4F_4$ would oppose the parallel shift of Cs and I, with either $Cs^+$ approaching $H^{\delta+}$ or $I^-$ approaching $F^{\delta-}$ thus increasing the energy. The Cs–F and I–H attractions together with Cs–H and I–F repulsions further bend the trapped molecule, from the carbon-skeleton folding angle of 162° in the free molecule to 150° in the complex.

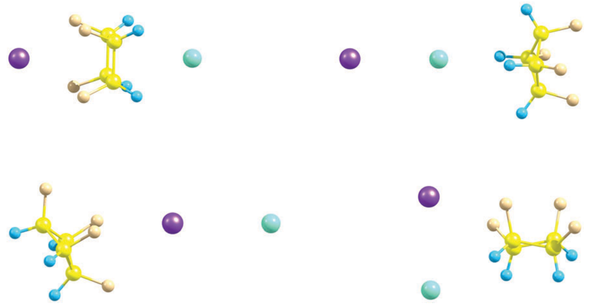

Fig. 2 Optimized geometries of the Cs–$C_4H_4F_4^{cis}$–I (trapped), CsI–$C_4H_4F_4^{cis}$ and $C_4H_4F_4^{cis}$–CsI (axial) and CsI:$C_4H_4F_4^{cis}$ (side) conformers.

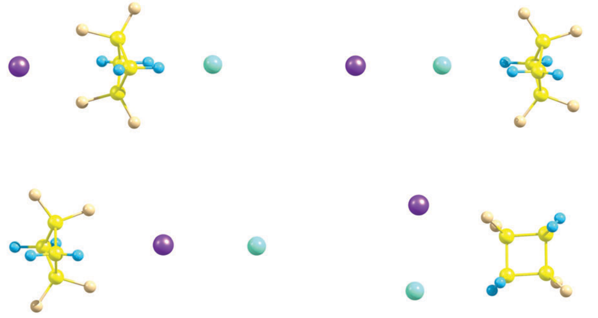

Fig. 3 Optimized geometries of the Cs–$C_4H_4F_4$–I (trapped), CsI–$C_4H_4F_4$ and $C_4H_4F_4$–CsI (axial) and CsI:$C_4H_4F_4$ (side) conformers, for the *cross* isomer of $C_4H_4F_4$.

Table 2 Equilibrium parameters (in eV and Å) of the studied systems

| System[a] | $D_e$[b] | $R_e$(Cs–F) | $R_e$(H–I) | $R_e$(Cs–I) |
|---|---|---|---|---|
| Cs–$C_4H_4F_4^{cis}$–I | 4.19, 0.60 | 2.94 | 2.92 | 6.66 |
| CsI–$C_4H_4F_4^{cis}$ | 4.16, 0.57 | | 2.85, 3.83 | 3.41 |
| CsI:$C_4H_4F_4^{cis}$ | 4.55, 0.96 | 2.98, 3.07 | 2.88, 3.13 | 3.49 |
| Cs–$C_4H_4F_4$–I | 2.98, −0.61 | 2.80 | 2.60 | 7.49 |
| CsI–$C_4H_4F_4$ | 3.95, 0.36 | | 2.95 | 3.40 |
| CsI:$C_4H_4F_4$ | 4.20, 0.61 | 3.13, 3.14 | 3.04, 3.47 | 3.42 |
| Cs–$C_4H_4F_4^{cis}$–$I^-$ | 1.81, 0.85 | 3.04–3.11 | 2.74, 3.58 | 7.40 |
| CsI–$C_4H_4F_4^{cis-}$ | 1.86, 0.90 | | 2.80, 3.77 | 3.64 |
| CsI:$C_4H_4F_4^{cis-}$ | 1.83, 0.87 | 3.44 | 2.59–3.86 | 3.72 |
| Cs–$C_4H_4F_4$–$I^-$ | 1.13, 0.17 | 3.03 | 2.73 | 7.84 |
| CsI–$C_4H_4F_4{}^-$ | 1.49, 0.53 | | 2.88 | 3.62 |
| CsI:$C_4H_4F_4{}^-$ | 1.45, 0.49 | 3.24, 3.29 | 3.03, 3.40 | 3.62 |
| Cs–$C_4H_4F_4^{cis+}$ | 1.04 | 2.98, 3.14 | | |
| $C_4H_4F_4^{cis}$–$I^-$ | 1.10 | | 2.78, 3.75 | |
| Cs–$C_4H_4F_4{}^+$ | 0.58 | 3.01 | | |
| $C_4H_4F_4$–$I^-$ | 0.64 | | 2.83 | |
| Cs–$C_4H_4F_4^{cis}$ | 0.27 | 3.18, 3.24 | | |
| $C_4H_4F_4^{cis}$–I | 0.15 | | 3.13 | |

[a] $C_4H_4F_4^{cis}$ and $C_4H_4F_4$ represent the all-*cis* and *cross* isomer, respectively; CsI–$C_4H_4F_4$ and CsI:$C_4H_4F_4$ represent the axial and side conformers, respectively. [b] Cs–mol–I → Cs + mol + $I^{(-)}$, → mol + $CsI^{(-)}$.

In contrast, the mutual attraction of the framing counter-ions, combined with the Cs–F and I–H interactions, flattens the carbon ring of the trapped all-*cis* molecule (originally part-folded at about 149°), unlike for Cs–$C_4H_8$–I[10] (with the molecule remaining slightly folded) but similar to the cases of lighter M–$C_4H_4F_4$–X.[8] So here both Cs and I are accommodated in the square hollows among, respectively, four F's and four H's. The most notable variations occur for the C–F bonds stretching by up 0.04 and 0.07 Å in the complexes for the all-*cis* and *cross* isomer, respectively, while the other bond lengths deviate within 0.01 Å.

The Cs–$C_4H_4F_4^{cis}$–I complex (with the all-*cis* isomer of the molecule) is bound by about 0.6 eV relative to isolated CsI and $C_4H_4F_4$, consistent with two strong ion–dipole interactions. The latter can be estimated as the difference between the total dissociation energy of the complex and that for the Cs–I pair at the separation in the complex, 4.19 − 1.61 = 2.58 eV, indicating a dominating contribution, similar to the (all-*cis* based) Cs–$C_6H_6F_6^{cis}$–I case.[6] In contrast, the structurally similar Cs–$C_4H_8$–I (with the nonpolar insert) is metastable, being about 0.5 eV higher in energy relative to CsI + $C_4H_8$.[10] The Cs–$C_4H_4F_4^{cis}$–I binding energy is smaller than the value of about 0.9 eV for the corresponding Cs–$C_6H_6F_6^{cis}$–I, consistent with the dipole moments of the trapped molecules ($\mu$ = 4.7 D and 5.9 D, respectively). Nevertheless, the binding is stronger than that for the lighter M–$C_4H_4F_4^{cis}$–X,[8] apparently due to the originally longer CsI being stretched relatively less by insertion.

The counterpart with the *cross* isomer is, however, metastable, being about 0.6 eV higher in energy than the corresponding dissociation products. This is apparently due to the stretch of the CsI by insertion of the weakly polar molecule (with $\mu$ = 0.92 D). The smaller dipole and thus weaker ion–dipole interactions (2.98 − 1.34 = 1.64 eV) result in the system energy increasing upon insertion even slightly more than for the Cs–$C_4H_8$–I case with a nonpolar insert, apparently due to the larger size of the trapped molecule and thus a longer (by 1.1 Å) stretch of CsI. In comparison, the Cs–$C_4H_4F_4^{cis}$–I system is about 0.8 Å shorter in terms of the Cs–I distance (Table 2). The latter system is also shorter than Cs–$C_6H_6F_6^{cis}$–I by about as much.

Three other, dipole–dipole conformers for each isomer of $C_4H_4F_4$ can be produced by attaching CsI axially by the Cs or I ends, or sideways, with Cs near F atoms and I near H's in every case (Fig. 2 and 3). For both isomers of $C_4H_4F_4$, the axial conformer with CsI attached by the I end is slightly more stable (by about 0.1 eV), even though $D_e$(HI) is significantly less than $D_e$(CsF) and the H–I distance in the complex exceeds $R_e$(HI) more compared to the CsF case. Still, this is consistent with the shorter internuclear separation in HI relative to CsF, translated into similar relations in the complexes and combined with shorter C–H bonds compared to C–F, thus leading to stronger interactions of the more closely spaced dipoles. Besides, $C_4H_4F_4^{cis}$–CsI with axial CsI is actually a transition state relaxing to off-axis CsI with Cs in the hollow between three F's. The axial CsI–$C_4H_4F_4$ conformer is near-degenerate with the marginally (by 0.03 eV) more stable Cs–$C_4H_4F_4$–I one for the all-*cis* isomer, while it is about 1 eV lower in energy and thus stable to dissociation by about 0.4 eV for the *cross* isomer of the molecule. To compare, the axial CsI–$C_6H_6F_6^{cis}$ conformer is slightly less stable than the Cs–$C_6H_6F_6^{cis}$–I one as well, although by 0.16 eV.[6] The side-attached CsI:$C_4H_4F_4$ conformer is found to be the most stable one for both isomers and bound by about 1 eV for the all-*cis* and 0.6 eV for the *cross* isomer, with CsI oriented, respectively, perpendicular and near-parallel to the edge

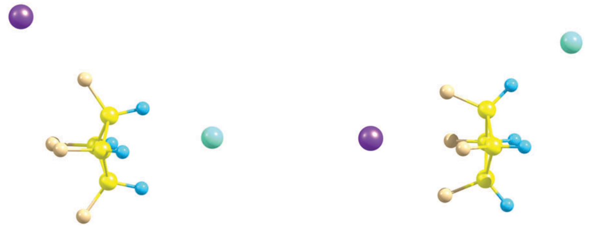

Fig. 4 Geometries of Cs–$C_4H_4F_4^{cis}$–I transition states towards Cs–I recombination.

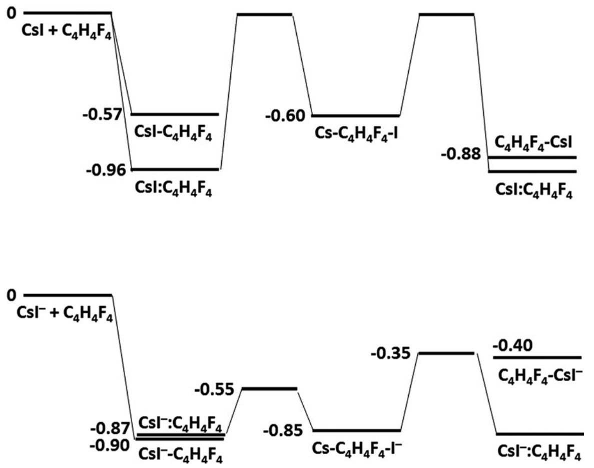

Fig. 5 Energy diagrams of the CsI + $C_4H_4F_4^{cis}$ (top) and $CsI^-$ + $C_4H_4F_4^{cis}$ systems.

of $C_4H_4F_4$. The Cs–I distances in these conformers follow the relative binding energies and stretch by 0.02 to 0.09 Å (Table 2).

The Cs–$C_4H_4F_4$–I complexes anticipated to have the largest dipole moments due to the longest Cs–I distance (as confirmed later below) are thus higher-energy conformers. The stabilizing potential energy barriers have been evaluated by gradually shifting the framing atoms off-axis and around the trapped molecule towards their recombination. During such a shift the relaxing all-*cis* $C_4H_4F_4$ recovers its part-folded shape, and either Cs or I prefer to move over a corner atom of the molecule, F or H, respectively (Fig. 4). The barrier heights are found to be near-equal in both cases at about 0.6 eV, thus levelling the transition states with the CsI + $C_4H_4F_4$ asymptote (Fig. 5). This is significantly larger than the value of under 0.2 eV for the $C_4H_8$-based counterpart,[10] apparently due to the strong ion–dipole interactions. The corresponding values for similar systems with $C_6H_6F_6$ are still higher, at about 0.7 and 1.0 eV,[6] apparently due to its larger dipole as well as size requiring a longer Cs–I separation to go around the molecule. For the case of *cross*-$C_4H_4F_4$, however, the barriers are considerably lower and close to that for the $C_4H_8$ case, at 0.3 and 0.1 eV for Cs and I, respectively, again consistent with the relative values of the molecular dipole moment and resulting interactions.

## 2- and 3-body interactions

To analyze the relevant binary interactions and to address other dissociation channels of the above complexes, the constituent atom–molecule pairs have been considered separately as well. In both Cs–$C_4H_4F_4^{cis+}$ and $C_4H_4F_4^{cis}$–$I^-$, the all-*cis* isomer of the molecule recovers its part-folded shape (Fig. 6), apparently due to the absence of the counter-ion on the opposite side and thus lack of the related compression. As another manifestation of this, in the binary cation Cs shifts off-axis into the hollow between three F-atoms, while in the binary anion I preserves its axial position. Both framing atoms remain axial for the *cross* isomer of $C_4H_4F_4$.

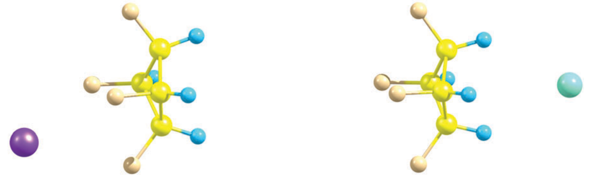

Fig. 6 Optimized geometries of Cs–$C_4H_4F_4^{cis+}$ and $C_4H_4F_4^{cis}$–$I^-$.

The ion–molecule binding energies are about 4 and 5 times less for the respective isomers than the total dissociation energy of Cs–$C_4H_4F_4$–I due to the absent ion–ion interactions, and are close for both Cs–$C_4H_4F_4^+$ and $C_4H_4F_4$–$I^-$ for each isomer (Table 2). The values for the all-*cis* isomer are about twice those for the *cross* one. Consistently, the ion–molecule distances increase (at least on average for the all-*cis* isomer). For comparison, the corresponding binding energies for the $C_6H_6F_6^{cis}$ case (1.24 and 1.47 eV) are somewhat larger, in accord with its larger dipole as well.[6] The differences between the total dissociation energy (adjusted to the ionic asymptote by adding IE(Cs)–EA(I)) and each binary one gives the energy for detachment of the other ion. This amounts to about 3.73 ± 0.03 and 2.98 ± 0.03 eV for the all-*cis* and *cross* isomer, respectively, reflecting their relative polarities. The former value is close to 3.75 ± 0.11 for $C_6H_6F_6^{cis}$.

Next, some corresponding neutral binary complexes have been studied. The binding energies of Cs–$C_4H_4F_4^{cis}$ and $C_4H_4F_4^{cis}$–I are about 4 and 7 times smaller than for their respective ions, consistent with their dipole-induced polarization character as compared to the above ion–dipole interactions. The higher value for the case of Cs is apparently due to its higher polarizability. The atom–molecule separations increase accordingly (Table 2). This allows us to calculate the detachment energies of the neutral Cs and I in Cs–$C_4H_4F_4^{cis}$–I as 3.92 and 4.04 eV, respectively, which, taking the above into account as well, suggests that the detachment of $Cs^+$ or $I^-$ is preferred. This is opposite to the case of isolated CsI as well as, *e.g.*, of Cs–$C_4H_8$–I (due to the weak binding in Cs–$C_4H_8$ and $C_4H_8$–I). The IE(Cs) – EA(I) difference, making Cs + I the preferred products for the latter cases, is more than compensated for Cs–$C_4H_4F_4^{cis}$–I by the strong ion–dipole attraction in the remainder.

In order to evaluate the non-additive 3-body interactions in the ternary system, its total binding energy can be compared with the sum of such values for the constituent pairs (2-body interactions), including each framing atom with the trapped molecule and two framing atoms. For consistency, all pairs are frozen in their geometries within the total complex.

Furthermore, two fragmentations can be compared, for the ionic and neutral atomic products: $Cs^+ + C_4H_4F_4 + I^-$ (correlating to the electronic structure of the complex) and $Cs + C_4H_4F_4 + I$ (the lower-energy dissociation channel). Then the atom–molecule pairs can be considered as ionic or neutral, respectively.

The sum of such ionic-pair interactions, $Cs^+–C_4H_4F_4$, $C_4H_4F_4–I^-$ and $Cs^+–I^-$ add up to 4.01 and 2.94 eV for the all-*cis* and *cross* isomers, respectively. This leaves 0.79 and 0.65 eV for the (thus cooperative) non-additive 3-body contributions. In the former case the two ion–dipole interactions together contribute near-equally with the ion–ion interaction which prevails (at about 2 : 1) in the latter case. In particular, such an extra stabilization is close to that for $Cs–C_6H_6F_6^{cis}–I$ (0.63 eV)[6] as well as for $Na–C_4H_4F_4^{cis}–F$ (0.72 eV).[8]

The neutral–pair interactions $Cs–C_4H_4F_4$, $C_4H_4F_4–I$ and Cs–I would sum up to 1.37 and 0.90 eV for the respective isomers, in which case the cooperative non-additive 3-body components dominate at 2.82 and 2.08 eV, respectively. This is about 3 times larger than for the previous case, and the former value is somewhat less than 3.2 eV for $Cs–C_6H_6F_6^{cis}–I$. The increase relative to the ionic products reflects the role of the charge-transfer in the stabilization of the system *via* the resulting ion–dipole interactions. The two (neutral) atom–molecule interactions contribute slightly repulsively at such distances but are strongly over-compensated by the stabilization of CsI relative to Cs + I due to the charge-transfer.

## Charges and dipoles

The atomic charges indicate a near-complete transfer of a single electron from Cs to I (Table 3). For the $Cs–C_4H_4F_4–I$ conformers the trapped molecule is charged more strongly, consistent with the charge going through it, while for the $CsI–C_4H_4F_4$ conformers, the charge is transferred beyond I. Interestingly, the less polar *cross* isomer carries a slightly higher charge of −0.15 *e*, the largest value among the systems studied here, while the all-*cis* isomer is charged equally to nonpolar $C_4H_8$.[8]

The complex with *cross*-$C_4H_4F_4$ has the largest dipole moment of more than twice that for CsI, consistent with the largest Cs–I distance, while for the shorter $Cs–C_4H_4F_4^{cis}–I$, the dipole is less by about a third, mainly due to the counter-directed contribution from the trapped molecule. For comparison, the value for $Cs–C_4H_8–I$ is between those for the two systems, again as a result of the interplay between the non-polarity of the trapped molecule and the Cs–I distance. In particular, by subtracting the difference of the dipole moments of Cs–I (at the distance in the complex) and $C_4H_4F_4$ from the total dipole, the induced-dipole component (including also the charge-transfer to the trapped molecule) can be estimated. For the all-*cis* and *cross* isomers of the molecule, this results in 18.5 − (30.6 − 4.7) = −7.4 and 26.4 − (34.9 − 0.9) = −3.6 D, respectively, showing a factor of 2 difference and (according to the signs) a prevailing polarization of the trapped molecule.

Table 3 Natural atomic charges and dipole moments (in *e* and *D*) of the studied systems

| System[a] | $q$(Cs) | $q$(H) | $q$(F) | $q$(I) | $\mu$ |
|---|---|---|---|---|---|
| $Cs–C_4H_4F_4^{cis}–I$ | 1.00 | 0.15–0.29 | −0.45, −0.48 | −0.90 | 18.5 |
| $CsI–C_4H_4F_4^{cis}$ | 0.98 | 0.19–0.22 | −0.37, −0.38 | −0.94 | 19.3 |
| $CsI{:}C_4H_4F_4^{cis}$ | 0.98 | 0.19–0.23 | −0.36–0.41 | −0.92 | 7.32 |
| $Cs–C_4H_4F_4–I$ | 1.00 | 0.23, 0.30 | −0.34, −0.47 | −0.85 | 26.4 |
| $CsI–C_4H_4F_4$ | 0.98 | 0.24, 0.27 | −0.37, −0.39 | −0.94 | 15.3 |
| $CsI{:}C_4H_4F_4$ | 0.97 | 0.25–0.28 | −0.37–0.41 | −0.94 | 11.5 |
| $Cs–C_4H_4F_4^{cis}–I^-$ | 0.05 | 0.20, 0.24 | −0.38–0.42 | −0.90 | |
| $Cs–C_4H_4F_4–I^-$ | 0.05 | 0.20, 0.24 | −0.38–0.42 | −0.90 | |

[a] $C_4H_4F_4^{cis}$ and $C_4H_4F_4$ represent the all-*cis* and *cross* isomer, respectively; $CsI–C_4H_4F_4$ and $CsI{:}C_4H_4F_4$ represent the axial and side conformers, respectively.

For the axial $CsI–C_4H_4F_4^{cis}$, both the polar components contribute additively, so the dipole is larger, even though only slightly – due to the much shorter Cs–I distance. Accordingly, for the corresponding complex with the *cross* isomer, the dipole is smaller by about the difference in its values between this and the all-*cis* isomer of $C_4H_4F_4$. In particular, by subtracting the sum of the $C_4H_4F_4$ and Cs–I dipole moments from that for the complex, the (predominantly) induced-dipole components could be estimated as 19.3 − (12.3 + 4.7) = 2.3 D and 15.3 − (12.3 + 0.9) = 2.1 D for the all-*cis* and *cross* isomers, respectively. Unlike for the above case, the values are close, in addition to being smaller.

The dipoles of the side-attached conformers are dominated by that of CsI, almost unchanged for the *cross* isomer (with its small dipole approximately perpendicular to that of CsI) or reduced by the counter-directed contribution from the all-*cis* isomer. The latter system has the smallest dipole of all studied here, almost a half that for CsI. Curiously, for each isomer the relative dipole values of the complexes follow the order opposite to that for their stabilities to dissociation.

In comparison, in $Cs–C_6H_6F_6^{cis}–I$ the trapped molecule carries the charge twice that in $Cs–C_4H_4F_4^{cis}–I$ and exceeding that in the complex with the *cross*-$C_4H_4F_4$. The dipole moments of both this and $CsI–C_6H_6F_6^{cis}$ conformers are larger (by about 2 D) than for those with the all-*cis* $C_4H_4F_4$, consistent with the longer Cs–I distance and larger dipole of all-*cis* $C_6H_6F_6$, respectively.[6] The induced dipoles of −8.9 D in $Cs–C_6H_6F_6^{cis}–I$ and 3.2 D in $CsI–C_6H_6F_6^{cis}$ are somewhat larger, apparently due to the higher polarizability of the larger molecule. The dipole moment of $Cs–C_4H_4F_4^{cis}–I$ exceeds those for the lighter $M–C_4H_4F_4^{cis}–X$ (up to 15.5 D),[8] apparently due to the longer Cs–I separation.

The electron densities at the bond critical points (within the AIM formalism[24]) of the complexes for the all-*cis* and *cross* isomers of $C_4H_4F_4$, calculated at the DFT/PBE0 level (with the same basis set), are collected in Table 4. The values for the Cs···F and H···I pairs are comparable and low, smaller by more than an order of magnitude than those for, *e.g.*, the C–F and C–H bonds (in the range of about 0.2–0.3 a.u.), thus indicating non-covalent interactions. In particular, the value for Cs···F in $Cs–C_4H_4F_4^{cis}–I$ is about same as that found for Na···F in $Na–C_4H_4F_4^{cis}–F$.[8] The lower densities for the conformers with attached CsI, especially for *cross*-$C_4H_4F_4$, are in accord with the longer Cs–F and H–I separations. In the corresponding anions the densities generally decrease, except for the H···I pair (especially for $CsI{:}C_4H_4F_4^{cis}$), in all cases consistent with the

Table 4 Electron densities at the selected bond critical points of the complexes

| System[a] | $\rho(\mathrm{Cs}\cdots\mathrm{F})$ | $\rho(\mathrm{H}\cdots\mathrm{I})$ |
|---|---|---|
| $\mathrm{Cs{-}C_4H_4F_4^{cis}{-}I}$ | 0.017 | 0.015 |
| $\mathrm{Cs{-}C_4H_4F_4{-}I}$ | 0.022 | 0.022 |
| $\mathrm{Cs{-}C_4H_4F_4^{cis}{-}I^-}$ | 0.011–0.013 | 0.016–0.017 |
| $\mathrm{Cs{-}C_4H_4F_4{-}I^-}$ | 0.013 | 0.017 |
| $\mathrm{CsI{:}C_4H_4F_4^{cis}}$ | 0.015 | 0.014 |
| $\mathrm{CsI{:}C_4H_4F_4}$ | 0.011 | 0.010 |
| $\mathrm{CsI{:}C_4H_4F_4^{cis-}}$ | | 0.022 |
| $\mathrm{CsI{:}C_4H_4F_4^-}$ | 0.009 | 0.011 |

[a] $\mathrm{C_4H_4F_4^{cis}}$ and $\mathrm{C_4H_4F_4}$ represent the all-*cis* and *cross* isomer, respectively $\mathrm{CsI{:}C_4H_4F_4}$ represent the side conformers.

opposite variations (general increase) of the corresponding atom–atom distances (Table 2). Curiously, in the anions these densities on the Cs side, where the extra electron is localized, become lower than on the I side.

## IR intensity spectra

The calculated IR-intensities for the all-*cis* $\mathrm{C_4H_4F_4}$ and its three conformers are collected in Fig. 7. For the isolated molecule, the two strongest lines near 1100 and 1200 $\mathrm{cm^{-1}}$ correspond, respectively, to the rocking of the carbon ring, accompanied by the antisymmetric stretch of the 1,3 C–F bonds and symmetric bending (wagging) of the 2′,4′ C–H bonds in counter-phase with carbons, and to the symmetric stretch of the carbon ring, accompanied by the symmetric bending of the C–H bonds (to-from the axis) and counter-phase stretching of the C–F bonds.

The spectrum varies rather weakly for the corresponding complex with the side-attached CsI, including mainly some weakening of the above lines while strengthening those near 800 $\mathrm{cm^{-1}}$. The two strongest of the latter lines correlate to the antisymmetric stretch of the carbon ring, accompanied by an antisymmetric stretch of the 1,3 F-bonds and symmetric bending of the 2′,4′ C–H bonds (in phase with carbons), and to the symmetric stretch of the carbon ring, accompanied by symmetric bending of the C–H bonds and in-phase stretching of the C–F bonds.

The axially attached CsI amplifies the above two strongest lines of the molecule, slightly for the lower- and more than twice for the higher-energy one. This difference is apparently due to the larger atomic shifts and thus dipole moment variation along the (axial) electric field of CsI for the latter vibrational mode. Both these lines are slightly red-shifted (by about 20 $\mathrm{cm^{-1}}$) in the complex. Such a variation of the spectrum is similar to that for the $\mathrm{CsI{-}C_6H_6F_6^{cis}}$ analogue.[6]

For $\mathrm{Cs{-}C_4H_4F_4^{cis}{-}I}$ the two dominant lines near 800 and 1100 $\mathrm{cm^{-1}}$ correspond to the symmetric stretch of the carbon ring (remaining flat), accompanied by symmetric bending of the C–H bonds (to-from the axis) and, respectively, in-phase or counter-phase stretching of the C–F bonds. The carbon ring thus axially moves, respectively, in counter-phase and in phase with hydrogens, making their amplitude and thus the dipole-moment variation (hence the line intensity) larger in the latter case. These lines are 5–7 times stronger than the corresponding ones for the isolated molecule, and red-shifted in the complex by about 100 $\mathrm{cm^{-1}}$. The intensity and shift increase as compared to the case with the axially attached CsI. In contrast, in the analogous case of $\mathrm{Cs{-}C_6H_6F_6^{cis}{-}I}$, the C–H bond stretch along the axis (rather than bending) generates a strong high-frequency line (near 3000 $\mathrm{cm^{-1}}$),[6] absent for the present system.

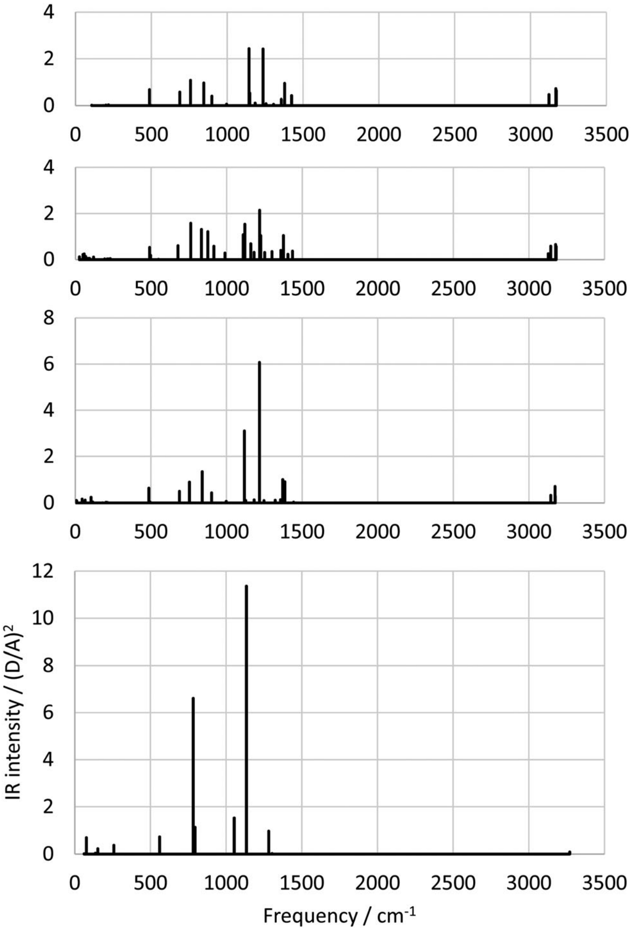

Fig. 7 IR intensity spectra of (top to bottom) $\mathrm{C_4H_4F_4^{cis}}$, $\mathrm{CsI{:}C_4H_4F_4^{cis}}$ (side), $\mathrm{CsI{-}C_4H_4F_4^{cis}}$ (axial), and $\mathrm{Cs{-}C_4H_4F_4^{cis}{-}I}$.

In the IR-intensity spectra of the *cross*-$\mathrm{C_4H_4F_4}$ isomer (Fig. 8), the two most (and near-equally) intense lines near 1200 and 1300 $\mathrm{cm^{-1}}$ correspond, respectively, to the folding of the carbon ring about the 1,3 C atoms and to the antisymmetric rocking of the opposite $\mathrm{C_2}$ units (with two others stretching). Both these vibrations are accompanied by the antisymmetric stretch of the C–F bonds and symmetric wagging (respectively perpendicular or parallel to the carbon ring) of the C–H bonds.

With the side-attached CsI, the corresponding vibrations remain IR-intense even though they weaken. For the first mode the line slightly red-shifts by about 20 $\mathrm{cm^{-1}}$, while the second mode evolves into an antisymmetric stretch of the carbon ring (hence involving all four $\mathrm{C_2}$ units) and slightly blue-shifts (by about as much). Moreover, there appears a much stronger line (by a factor of 2–3) near 3000 $\mathrm{cm^{-1}}$, dominated by the symmetric stretch of the $\mathrm{CH_2}$ group nearer to CsI, with the highest-amplitude vibrations of the H atom pointing (approximately) to I.

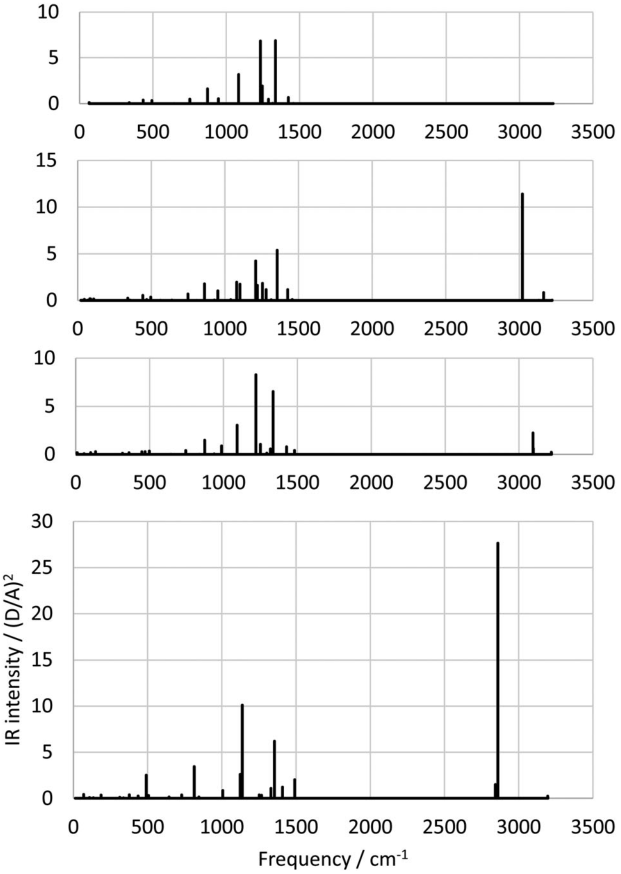

Fig. 8 IR intensity spectra of (top to bottom) $C_4H_4F_4$, CsI:$C_4H_4F_4$ (side), CsI–$C_4H_4F_4$ (axial), and Cs–$C_4H_4F_4$–I for the *cross* isomer of the molecule.

When CsI is attached axially, the above two modes of the isolated molecule preserve or even increase their IR intensities, and show almost no shift. The high-frequency mode occurs near 3100 cm$^{-1}$ and corresponds to the in-phase symmetric stretch of both $CH_2$ groups. For this mode, in each such group one H atom shifts to and the other from CsI, thus moderating the dipole alteration. In accord, the intensity of the line is much lower – by about 3–4 times relative to the most intense lines and up to 5 times as compared to the above high-frequency analogue for the side-attachment case.

For the Cs–$C_4H_4F_4$–I complex the three above modes persist as the most IR-intense, although with some variations in the relative line strengths and positions. The lines correlating to the two isolated-molecule vibrations again red- and blue-shift by about 100 and 20 cm$^{-1}$, respectively, and approximately preserve the intensities found for the axially-attached complex. The high-frequency mode is, however, an order of magnitude more IR-intense and red-shifted by about 250 cm$^{-1}$ relative to the axially-attached CsI case. Such a dramatic increase could be attributed to the higher-amplitude motions of the H-atoms pointing along the axis, as well as to the stronger interaction of the molecular dipole with the framing ion-pair, with both ions equally and cooperatively involved – in this dipole-inside-of-dipole rather than the dipole-near-dipole arrangement.

Curiously, the overall evolution of the IR-spectra from the isolated molecule to CsI–$C_4H_4F_4$ to Cs–$C_4H_4F_4$–I shows a similarity between the systems with *cross*-$C_4H_4F_4$ and all-*cis* $C_6H_6F_6$, while those with all-*cis* $C_4H_4F_4$ differ. This could perhaps be related to the higher rigidity of the former two molecules, leading to the larger role of the high-frequency C–H stretch resulting in the most prominent lines, while the more flexible last molecule (altering its shape in Cs–$C_4H_4F_4$–I) more actively involves the lower-frequency vibrations of the C atoms.

### Triplet states

In the triplet state, with Cs and I essentially neutral (as in isolated CsI), the Cs–$C_4H_4F_4^{cis}$–I complex bends, with the molecule recovering its part-folded geometry and Cs shifting off-axis into the hollow between three F atoms. The Cs–I distance stretches by about 1.4 Å, with the Cs–F and H–I distances increasing about equally. The total dissociation energy drops to 0.45 eV and is apparently due to the polarization of the framing atoms by the molecular dipole. This is consistent with the overall dipole moment of 8.6 D still being significantly larger than that of the isolated molecule, indicating a considerable contribution of the induced components on the framing atoms. It is worth noting that the dipole is inverted in direction relative to the singlet state, in accord with the orientation of the polar molecule. For the other conformers, the attached CsI strongly stretches in the triplet state, in accord with the relevant behaviour of the isolated molecule.

The above alterations are generally similar to those for Cs–$C_6H_6F_6^{cis}$–I, except for its somewhat larger binding energy (about 0.7 eV) and smaller stretch (by about 0.9 Å) in the triplet state. This and the larger inverted dipole (about 13 D) are consistent with the large dipole of the molecule.

For the *cross*-$C_4H_4F_4$ isomer, the triplet-state complex exhibits a similar evolution, stretching by about 1.0 Å in the Cs–I distance but remaining linear. The total dissociation energy reduces to 0.23 eV, and the dipole moment diminishes.

### Anions

The anions of the complexes mainly preserve the geometries of the neutral parents, in particular for all conformers of *cross*-$C_4H_4F_4$. Exceptions occur for Cs–$C_4H_4F_4^{cis}$–I$^-$ and its conformer with side-attached CsI. For the former, with the cationic Cs essentially neutralized (as discussed further below), the weaker Cs–I$^-$ attraction is insufficient to keep the trapped molecule flat. It therefore recovers its part-folding (Fig. 9), and Cs shifts into the hollow between three F atoms, similar to the triplet-state case above. As a result, the Cs–I distance increases by about 0.7 Å (Table 2). The total dissociation energy drops more than twice relative to the neutral system, since the ion–dipole and ion–ion interactions are replaced by the weaker atom–dipole and atom–ion ones. However, the stability relative to separated CsI$^-$ and $C_4H_4F_4^{cis}$ increases from the neutral case by 0.25 eV, apparently due to the even larger destabilization of the isolated diatom (by about 2.6 eV in the dissociation energy).

The axially-attached conformer exhibits similar variations in stability, remaining almost equally stable compared to Cs–$C_4H_4F_4^{cis}$–I$^-$, with the binding energy only marginally larger (by 0.05 eV).

**Fig. 9** Optimized geometries of the Cs–$C_4H_4F_4^{cis}$–$I^-$ (trapped) and CsI:$C_4H_4F_4^{cis-}$ (side) conformers.

The attached diatom is about 0.2 longer than in the neutral counterpart and the I end is slightly closer to the molecule (Table 2). The least bound conformer with CsI attached by the Cs end is further destabilized due to the neutralization of Cs, so that the binding energy becomes still smaller than for the previous case (by about 0.5 eV). In the corresponding side-attached conformer, CsI again stretches by about 0.2 Å relative to the neutral system and slides around the molecule so that I is in the near-axial position (Fig. 9). Upon electron attachment the stability to the total dissociation reduces more strongly than for the other conformers, while the binding energy reduces by about 0.1 eV, so that this conformer becomes almost degenerate with Cs–$C_4H_4F_4^{cis}$–$I^-$ and the axially-attached counterpart.

The situation is different for the respective complexes of *cross*-$C_4H_4F_4$. The total dissociation energies drop almost 3 times for all conformers, and the axially and side-attached ones become near-degenerate (Table 2). The stability relative to $CsI^-$ + $C_4H_4F_4$ increases significantly for Cs–$C_4H_4F_4$–$I^-$, making it slightly stable (by about 0.2 eV) in contrast to the metastable neutral system, similar to the situation for the case of nonpolar $C_4H_8$.[10] The binding energies become near-equal in the conformers with the attached diatom, at about 0.5 eV. The Cs–I stretch upon electron attachment is again larger for Cs–$C_4H_4F_4$–I, but less than for the case of the all-*cis* isomer, consistent with the smaller dipole.

For Cs–$C_4H_4F_4^{cis}$–$I^-$, the potential energy barriers for Cs or I to go around the molecule towards the other framing atom and form the attached diatom are about 0.3 and 0.5 eV, respectively, *i.e.* lower than for the neutral system, apparently due to the weaker Cs–$I^-$ interaction. Now the transition states are below the $CsI^-$ + $C_4H_4F_4^{cis}$ asymptote (Fig. 5). The corresponding values for the *cross*-$C_4H_4F_4$ case are still smaller, at about 0.1 and 0.2 eV. In both cases, the neutralized Cs atom has a lower barrier, consistent with its weaker interaction with the molecular dipole. For the latter case the slight increase of the I-barrier compared to the neutral system could be related to the absence of the accompanying shift of Cs observed in the neutral system.

For both isomers of $C_4H_4F_4$, the extra electron in the anions concentrates predominantly on Cs, making it almost neutral (Table 3). Only $-0.15\,e$ resides on the trapped molecule for both isomers, which is about same as for the neutral system.

The electron affinities of the systems can be calculated as EA = EA(I) + $D_e^{\text{total}}$(anion) – $D_e^{\text{total}}$(neutral). The values are rather low, ranging from 0.4 to 1.3 eV, their variations are governed by the $D_e^{\text{total}}$(neutral) values and correlate to the dipole moments (Table 5). The side-attached conformers thus have the lowest EA which is even less than EA(CsI) = 0.51 eV, while the largest value belongs to Cs–$C_4H_4F_4$–I with the *cross* isomer of the molecule and is almost the same as for Cs–$C_4H_8$–I (1.2 eV).[10]

**Table 5** Electron affinities (in eV) of the neutral complexes (=adiabatic electron-detachment energies of their anions)

| Conformer | all-*cis* $C_4H_4F_4$ | *cross* $C_4H_4F_4$ |
|---|---|---|
| Cs–$C_4H_4F_4$–I | 0.76 | 1.29 |
| CsI–$C_4H_4F_4$ | 0.84 | 0.68 |
| CsI:$C_4H_4F_4$ | 0.42 | 0.39 |

## Conclusions

Presented is a systematic computational study of several conformers of the CsI + (cyclic) $C_4H_4F_4$ system for different isomers of the tetrafluoro-cyclobutane, and the corresponding anions. In addition to the conventional dipole–dipole complexes with various mutual orientations of the attached polar components, the uncommon dipole-inside-of-dipole, Cs–$C_4H_4F_4$–I species with the atomic counter-ions trapping the molecule have been investigated. Due to the electron density and charge distribution features, such unique species could be formed by two out of several considered isomers of $C_4H_4F_4$, 11′33′- (*cross*) and 1234-fluorinated (all-*cis*). Their comparison, including also the previously studied analogous complexes of cyclic $C_4H_8$, shows the evolution of the properties of structurally similar systems with increasing polarity.

The conformers with the side-on attachment of CsI and $C_4H_4F_4$ (with counter-directed dipoles) are found to be most stable for both the all-*cis* and *cross* isomers. This confirms the limited applicability of the point-dipole predictions for such systems, apparently due to the comparable separations of the ions in and between the dipoles. Furthermore, the uncommon Cs–$C_4H_4F_4$–I conformer can be metastable or degenerate and even more stable relative to the usual CsI–$C_4H_4F_4$ one, as found for the *cross*- and all-*cis* $C_4H_4F_4$, respectively. Moreover, the potential energy barriers stabilizing the former conformer can be significantly higher for the all-*cis* than for the lower-energy *cross*-$C_4H_4F_4$, thus increasing its formation probability and lifetime.

The electron-attachment is predicted to affect the relative stabilities of the different conformers differently and to level out the stabilities of the corresponding anions, up to their near-degeneracy for all-*cis* $C_4H_4F_4$. In addition, the barriers between the anions are reduced, in particular well below the $CsI^-$ + $C_4H_4F_4^{cis}$ asymptote, unlike for the neutral system. This suggests an increased probability of formation of Cs–$C_4H_4F_4^{cis}$–$I^-$ *via* a direct interaction (collision) of $CsI^-$ and $C_4H_4F_4^{cis}$. Alternatively, this conformer could be produced, *e.g.*, starting with the (most stable, hence readily formed) side-attached CsI:$C_4H_4F_4$, then making its anion which may transform to the near-equally bound Cs–$C_4H_4F_4^{cis}$–$I^-$ over the 0.3 eV barrier. In particular, the anionic systems can be dealt with more readily by means of mass-spectrometry.

Next, once the above anion is produced in either way, photodetachment of the extra electron could lead to the higher-energy Cs–$C_4H_4F_4^{cis}$–I conformer stabilized by about 0.6 eV barriers and thus sufficiently stable at low temperatures. Still another probable route could be a stepwise ion-attachment, *i.e.* $Cs^+$ + $C_4H_4F_4^{cis}$ followed by Cs–$C_4H_4F_4^{cis+}$ + $I^-$, or the other way around, with both steps being exothermal. Also, the (exothermal) interaction of the $C_4H_4F_4^{cis}$–$I^-$ intermediate with Cs might also result in Cs–$C_4H_4F_4^{cis}$–$I^-$ to be neutralized by electron photo-detachment.

When the system of interest is formed, it could be detected and analyzed by means of the IR spectroscopy. The calculated IR intensity spectra exhibit sensitivity to both the conformer structure and the constituent $C_4H_4F_4$ isomer, thus enabling a reliable differentiation between the complexes. In particular, the Cs–$C_4H_4F_4$–I species are clearly "advertised" by the strongest spectral lines among all conformers, originating from either strong or weak lines in the isolated $C_4H_4F_4$ (all-*cis* or *cross*, respectively). The highest intensities belong to the vibrational modes with the atoms of the trapped molecule moving axially between the framing ions.

Besides, the IR spectra can show larger intensity variations with the mutual orientation of the polar molecular components than with their binding energies. For instance, side-attached CsI:$C_4H_4F_4^{cis}$ is bound more strongly than axially-attached CsI–$C_4H_4F_4^{cis}$ which, however, exhibits larger alterations in the spectrum relative to the isolated molecule, apparently due to the much larger dipole.

## Conflicts of interest

There are no conflicts of interest to declare.

## Acknowledgements

This work was financed by the UOIT Summer Employment Program and the Faculty of Science. Calculations have been carried out on the HPC facilities of this Faculty and the SHARCNet of Ontario, and we are grateful to their staff for technical support.

## References

1 N. Camaioni and R. Po, *J. Phys. Chem. Lett.*, 2013, **4**, 1821.
2 P. Wang, P. Zhu, W. Wu, H. Kang and C. Ye, *Phys. Chem. Chem. Phys.*, 1999, **1**, 3519.
3 N. S. Keddie, A. M. Z. Slawin, T. Lebl, D. Philp and D. O'Hagan, *Nat. Chem.*, 2015, **7**, 483.
4 B. E. Ziegler, M. Lecours, R. A. Marta, J. Featherstone, E. Fillion, W. S. Hopkins, V. Steinmetz, N. S. Keddie, D. O'Hagan and T. B. McMahon, *J. Am. Chem. Soc.*, 2016, **138**, 7460.
5 S. A. C. McDowell, *Comput. Theor. Chem.*, 2017, **1108**, 18.
6 F. Y. Naumkin, *J. Phys. Chem. A*, 2017, **121**, 4545.
7 C. Trujillo, G. Sanchez-Sanz, I. Alkorta and J. Elguero, *J. Phys. Chem. A*, 2011, **115**, 13124.
8 S. A. C. McDowell, *Chem. Phys. Lett.*, 2016, **665**, 105.
9 G. Kochhar and F. Y. Naumkin, *New J. Chem.*, 2010, **34**, 2932.
10 B. Cochrane and F. Y. Naumkin, *Chem. Phys. Lett.*, 2016, **643**, 137.
11 F. Y. Naumkin, *Phys. Chem. Chem. Phys.*, 2008, **10**, 6986.
12 C. Garau, D. Quiñonero, A. Frontera, P. Ballester, A. Costa and P. M. Deyà, *New J. Chem.*, 2003, **27**, 211.
13 I. Alkorta and J. Elguero, *J. Phys. Chem. A*, 2003, **107**, 9428.
14 I. Alkorta, F. Blanco, P. M. Deya, J. Elguero, C. Estarellas, A. Frontera and D. Quinonero, *Theor. Chem. Acc.*, 2010, **126**, 1.
15 A. Frontera, D. Quinonero and P. M. Deya, *Wiley Interdiscip. Rev.: Comput. Mol. Sci.*, 2011, **1**, 440.
16 Z. Fang, N. Al-Maharik, A. M. Z. Slawin, M. Bühl and D. O'Hagan, *Chem. Commun.*, 2016, **52**, 5116.
17 A. J. Durie, A. M. Z. Slawin, T. Lebl, P. Kirsch and D. O'Hagan, *Chem. Commun.*, 2011, **47**, 8265.
18 A. J. Durie, A. M. Z. Slawin, T. Lebl, P. Kirsch and D. O'Hagan, *Chem. Commun.*, 2012, **48**, 9643.
19 K. L. Schuchardt, B. T. Didier, T. Elsethagen, L. Sun, V. Gurumoorthi, J. Chase, J. Li and T. L. Windus, *J. Chem. Inf. Model.*, 2007, **47**, 1045. https://bse.pnl.gov/bse/portal.
20 M. Valiev, E. J. Bylaska, N. Govind, K. Kowalski, T. P. Straatsma, H. J. J. van Dam, D. Wang, J. Nieplocha, E. Apra, T. L. Windus and W. A. de Jong, *Comput. Phys. Commun.*, 2010, **181**, 1477.
21 *CRC Handbook of Chemistry and Physics*, 88th edn, 2007.
22 *NIST Chemistry WebBook, NIST Standard Reference Database Number 69*, ed. P. J. Linstrom and W. G. Mallard, NIST, Gaithersburg MD, 2017, p. 20899, http://webbook.nist.gov/chemistry/.
23 A. E. Reed, L. A. Curtiss and F. Weinhold, *Chem. Rev.*, 1988, **88**, 899.
24 R. F. W. Bader, *Atoms in Molecules: A Quantum Theory*, Oxford Univ. Press, Oxford, 1990.